

Design and Manufacturing of a High Torque PMSM with Tooth-Coil Winding and Solid Rotor Yoke

Nicolas Erd
Institute of Electrical Energy Conversion
TU Darmstadt
 Darmstadt, Germany
 nerd@ew.tu-darmstadt.de

Andreas Binder
Institute of Electrical Energy Conversion
TU Darmstadt
 Darmstadt, Germany
 abinder@ew.tu-darmstadt.de

Abstract—The mechanical design and manufacturing process of a high-torque, outer rotor PMSM with tooth-coil winding and solid rotor yoke is presented. Throughout the design process the principle of modularisation is applied for efficient construction of this rather large machine in the context of university equipment and workshops.

Keywords—tooth-coil winding, prototype manufacturing, outer rotor, PMSM

I. INTRODUCTION

The regarded machine is a downsized prototype of a direct-drive PMSM wind generator with tooth-coil winding and solid rotor yoke [1]. The purpose of the prototype is to test the combination of a tooth-coil winding with a solid rotor yoke, which is problematic due to the significant space harmonics and sub-harmonics evoked by a tooth-coil winding leading to rotor eddy currents [2, 3, 4]. But for high torque, low speed and low stator frequency applications, which are found in gearless drive systems, the rotor eddy current losses may be overcompensated by the decrease of ohmic stator losses due to very short winding overhangs and the inherent possibility to economic modularisation. Consequently large gearless wind generators are a suitable application [5, 6, 7, 8, 12].

The dimensions of the downsized prototype treated here are: 700 mm outer diameter and 90 mm active length. The nominal torque is 2800 Nm at a nominal speed of 60 min^{-1} or 120 min^{-1} at $U_N \approx 400 \text{ V}$ (switchable number of parallel branches). The machine features an outer rotor design, internal water jacket cooling and a prefabricated, form-wound, three phase, double layer tooth-coil round wire winding with a number of slots per pole and phase of $q = 2/5$. The main machine dimensions and 2D-FEM-simulation results of nominal operation at $n = 60 \text{ min}^{-1}$ are provided in Tab. 1.

Since the terminals of all principal winding schemes of the prototype machine are lead through the housing, different nominal speeds (60 min^{-1} or 120 min^{-1}) are available at similar nominal voltage. This enables an experimental investigation of rotor eddy current losses in a rather broad stator frequency range without field weakening. Further the external interconnection will be used to feed only sections of the stator winding leaving parts of the stator winding idling. This operation mode is used in large drive high pole count machines, which have parallel branches fed from separate inverters to establish redundancy operation in case of a single inverter failure. However this operation comes with additional stator field space harmonics, especially large sub-harmonics reaching the solid rotor yoke easily, and can cause significant rotor losses [1, 9, 10, 12].

This paper will focus on the machine design and prototype manufacturing. The construction design follows the principle of modularisation strictly and thereby it was

possible to carry out most of the production steps in the university workshops. In section II the general machine design is outlined and the main assembly steps are briefly described. Section III deals with the manufacturing of the winding. And section IV describes the test bench setup before the paper is summarised in the conclusion.

TABLE I. MACHINE DIMENSIONS AND SIMULATION OF NOMINAL OPERATION (JMAG 20.0 [X])

Parameter	Value
Number of slots per pole and phase q	2/5
Poles $2p$	40
Axial stack length l_{fe}	90 mm
Stator inner/outer diameter	400 mm / 658 mm
Rotor yoke inner/outer diameter	679 mm / 700 mm
Magnet height / min. air gap	8.5 mm / 2.0 mm
Thermal class	180 (H)
Max. magnet temperature	100°C
Speed	60 min^{-1}
Torque	2828 Nm
Mechanical power	17.77 kW
Stator frequency	20 Hz
Stator fundamental phase current I_1	35.01 A
Stator fundamental phase voltage U_1	190.4 V
$\cos(\varphi_1)$	0.7438 (ind.)
Total losses	2895 W (100%)
AC-copper losses	2487 W (86%)
Stator iron losses	223 W (8%)
Eddy current losses: rotor magnets	40 W (1%)
Eddy current losses: rotor yoke	145 W (5%)
Generator efficiency η	83.70%

II. MACHINE DESIGN

The prototype is shown in Fig. 1 in sectional view in order to provide an insight to the internal components, such as the stator core and tooth-coil winding as well as the internal stator support.

A. Stator Support

The stator support is the central structural element with the following functions:

- i. Fixation of the machine via flange to the mount on the B-side. The mount (⑦ in Fig. 1) is the final support to the foundation.
- ii. Internal water cooling jacket with water connections on the B-side. The meandering cooling channel is formed by axial drill holes with alternating sectorial connection millings. The resulting water cavity is closed by two lids on the A- and B-side. A free cut of the cavity is provided in Fig. 2.

- iii. Support of the stator core yoke by a twelvefold keyed joint: Axial keyseats are milled to the stator support between the cooling channels. The stator core yoke has the corresponding twelve teeth of the joint.
- iv. Seat for the bearing system of the outer rotor on the A-side. A commercially available integrated wheel bearing is used (*SKF* [xvii] *VKBA 6666*).
- v. Central whole for the encoder shaft.
- vi. Mount for the incremental encoder (*SICK* [xvi] *DFS60A 16 Bit*) buried on the B-Side (⑤ in Fig. 1).

This component is manufactured from a single piece of 7075-T6 aluminium, which is lightweight, high-strength and easy to machine (Fig. 3).

B. Stator Core and Winding

The active stator components consist of the laminated core and the winding. The core consists of a single yoke ring and 48 individual tooth cores manufactured by *Nestech* [xiii]. Each tooth is insulated by an insulation paper (0.3 mm Nomex-Kapton-Nomex composite) (Fig. 4) and equipped with a prefabricated coil. Due to the parallel sided tooth the coil slides on the teeth from the inner side (Fig. 5). Then the tooth axially slides into the dovetail joint of the yoke ring (Fig. 6). The double layer winding consist of different coils for the upper and lower layer, differing in outer dimensions and number of turns. The coils are placed on top of each

other. Compared to the side by side arrangement the slot area spend on inter-phase insulation is drastically minimized since the depth of the slot is larger than the slot width. The completely assembled stator is shown in Fig. 7. The interconnection, installation of thermistors (26 three-wire PT100) and immersion impregnation (*Elantas* [iv] *EpoxyLite H1100*) is realized by *Brenner* [ii] (Fig. 8).

C. Rotor and Magnet Assembly

The rotor consists of a solid steel yoke from S355 mild steel and is produced by *Volkmann* [xviii] as a welded construction of a seamless tube and lid. The NdFeB-permanent magnets acquired from *Magnetworld* [xi] are three times axially segmented per pole and each of the 120 magnet segments (three times 40 poles) is a cuboid of the size 30 mm x 43 mm x 8.5 mm (axial length x width x height). The magnets are positioned in 2 mm deep slots, which provide lateral guidance. The magnets are fixated by two-component epoxy resin (*Henkel UHU Plus Endfest 300*). The epoxy is cured for 1.5 hours at 75°C heated by a heating pad fixed to the outer rotor surface. The epoxy resin and curing scheme limit the rotor temperature to 100°C. The magnets are assembled fully magnetized and are inserted and hold in place during curing by a lead screw jig (Fig. 9 and 10). A 0.3 mm thick metal sheet is used in order to slide the magnet over the previously applied resin. The sheet will be retracted by pulling on the clamping bars attached to it. All jig components are manufactured from unmagnetic metals.

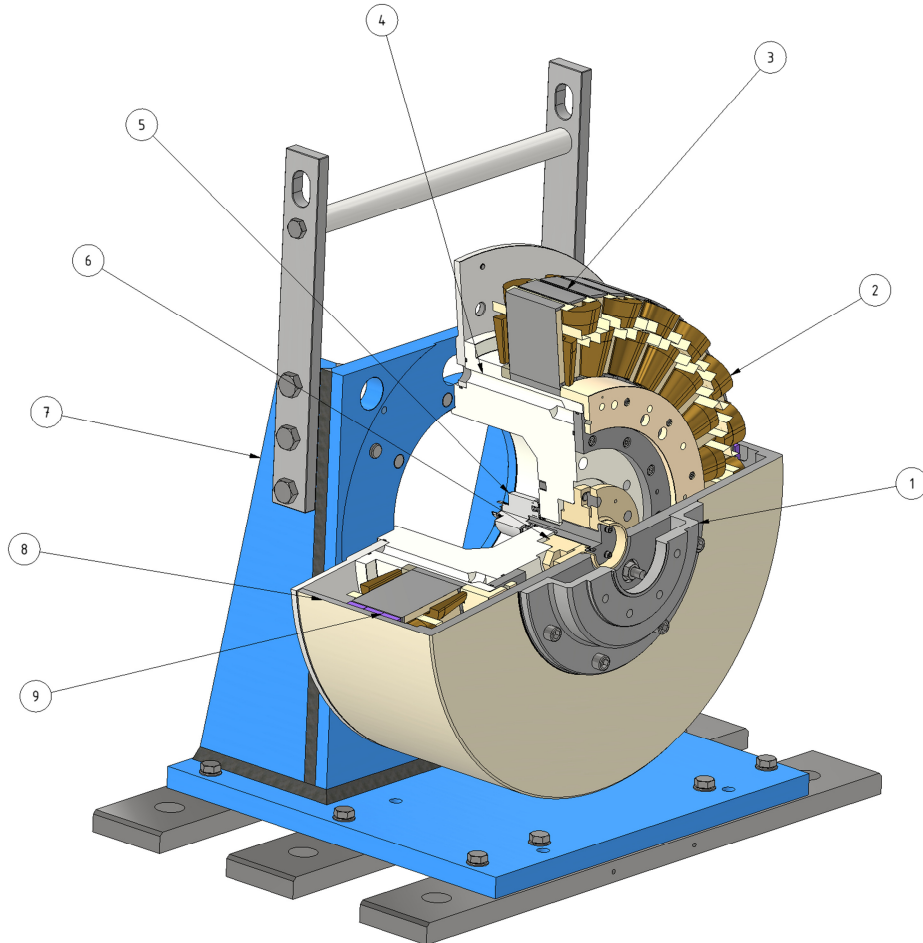


Fig. 1 3D-CAD-model (*Inventor* [i]) of the prototype machine; rotor in half-section; stator in three-quarter-section; A-side in front; B-side on the back: ① coupling flange; ② form-wound tooth-coil; ③ single tooth iron package; ④ stator support with internal water jacket; ⑤ incremental encoder; ⑥ bearing; ⑦ flange mount; ⑧ solid rotor yoke; ⑨ segmented magnets

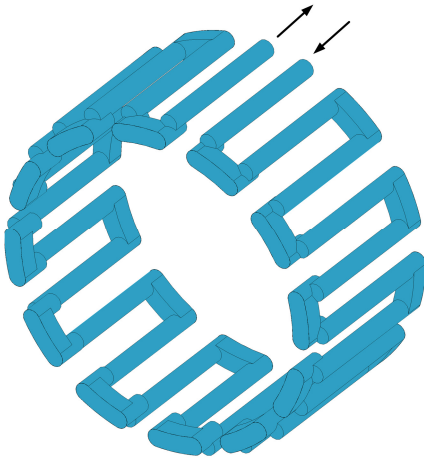


Fig. 2 3D-CAD free cut (*Inventor [i]*) of the internal cooling water jacket; arrows show inflow and outflow



Fig. 3 Stator support after machining.

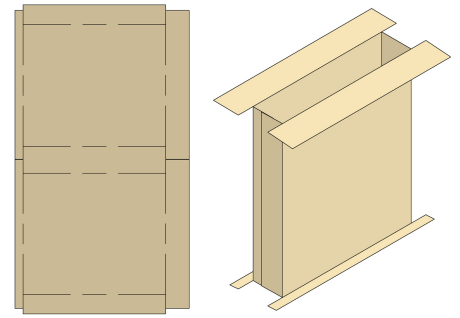


Fig. 4 3D-CAD-model (*Inventor [i]*) of the main slot insulation wrapped around each tooth; left: flat pattern; right: folded insulation

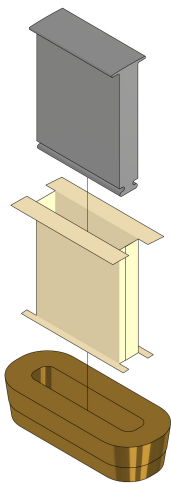


Fig. 5 3D-CAD-model (*Inventor [i]*) of the preassembly of one tooth, main insulation and coil

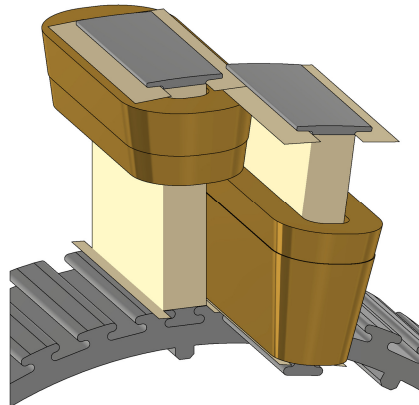


Fig. 6 3D-CAD-model (*Inventor [i]*) of the stator assembly by axial insertion of individual teeth with preassembled coil



Fig. 7 Assembled stator prior to interconnection and impregnation on mounting support (blue)



Fig. 8 Stator interconnection prior to impregnation, both carried out by *Brenner [ii]*

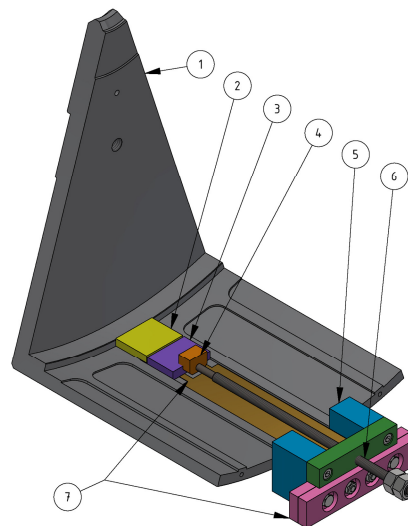


Fig. 9 3D-CAD-model (*Inventor [i]*) of the leadscrew jig: ① sectorial cut of the rotor; ② spacer; ③ cuboid magnet segment; ④ lead screw adapter; ⑤ jig mount screwed to the rotor; ⑥ lead screw and thread bar; ⑦ slide sheet and clamping bars

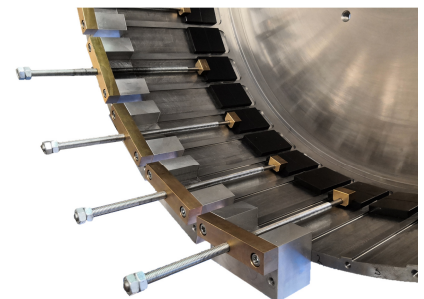


Fig. 10 PM mounting; second axial segments are mounted; five magnets are mounted in one sequence

III. WINDING

A. Design

The stator winding consist of 24 upper layer and 24 lower layer prefabricated, form-wound coils of enamel round wire (*SHWire* [xiv] *SHTherm 210*) with different number of turns as shown in Tab. 2. Each principal winding scheme consist of a series connection of one lower layer coil and one neighbouring upper layer coil (Fig. 11). The number of parallel branches can be chosen as $a = 4$ for $n = 60 \text{ min}^{-1}$ and $a = 8$ for $n = 120 \text{ min}^{-1}$ in an external cabinet.

B. Manufacturing

The coils are manufactured in the winding workshop of the institute on a linear winder (Fig. 12) with a tension-controlled wire feeder (Fig. 13) based on a current-controlled DC drive. Two machined moulds, one for the lower layer (Fig. 18, 23) and one for the upper layer, are used to ensure correct inner and outer dimensions of the coil and an orthocyclic winding pattern. During the winding process the side plates (④ in Fig. 23) are removed and the wire is wound around the split core (② in Fig. 23). For precise winding results the wire feeding in the baseplate is crucial: Fig. 14 and 15 show the ramp feeding design to the winding overhang, which ensures that the repositioning of the wire at the beginning (Fig. 14), after completion of a turn (Fig. 15) and after completion of a layer takes place in the winding overhang without affecting the confined slot space. The winding process is wet, i. e. each layer is manually impregnated by a filled two-component slow curing epoxy resin (*Elantas* [iv] *Elan-tron MC5430/W5868*).

After completion of the winding process and before curing the side moulds are installed to ensure precise outer coil dimension (④ in Fig. 23). The impregnated coil is cured at 60°C in an oven under constant low speed rotation of 2.5 min^{-1} around the horizontally aligned winding axis. After curing, the finished coil (Fig. 19) can be demoulded flawlessly by taking apart the side mould and inner mould. This process is supported by the split core design, which releases

wire tension build up during the winding process by sliding on the diagonal face inwards. Further the mould is regularly treated by a spray wax as a mould release agent (*Elantas* [iv] *Z 25 LE*).

This winding process leads to almost orthocyclic windings disturbed only by the relatively large outer contour. The copper fill factors related to the mould cross sections are 0.658 for the lower mould and 0.700 for the upper mould (wire tapering due to winding process is taken into account). The overall copper fill factor related to the complete slot area (with slot-opening and all insulation) is 0.553. The correct winding pattern is checked through fabrication of a three-quarter-cut demonstration coil (Fig. 20). The polished cut face (Fig. 21) shows the orthocyclic winding pattern. Note that the additional transparent resin is only used for this cutaway.

The high copper fill and the impregnation during the winding with high resin fill leads also to high transverse thermal conductivity. Consequently air pockets on the outer coil contour and the slot liner become the main thermal resistances in the cooling path of copper loss towards the cooled iron core (Fig. 22). The thermal calculation may be found in [13].

TABLE II. WIRE AND WINDING PARAMETERS

Parameter	Value
Nominal wire diameter (blank) $d_{\text{Cu},o}$	1.8 mm
Mean wire diameter after winding (blank) d_{Cu}	1.716 mm
Insulation grade	2
Thermal class	200
Upper coil: number of turns	198
Lower coil: number of turns	207
Copper fill factor related to the mould area lower/upper	0.658/0.700
Overall copper fill factor related to the slot area	0.553

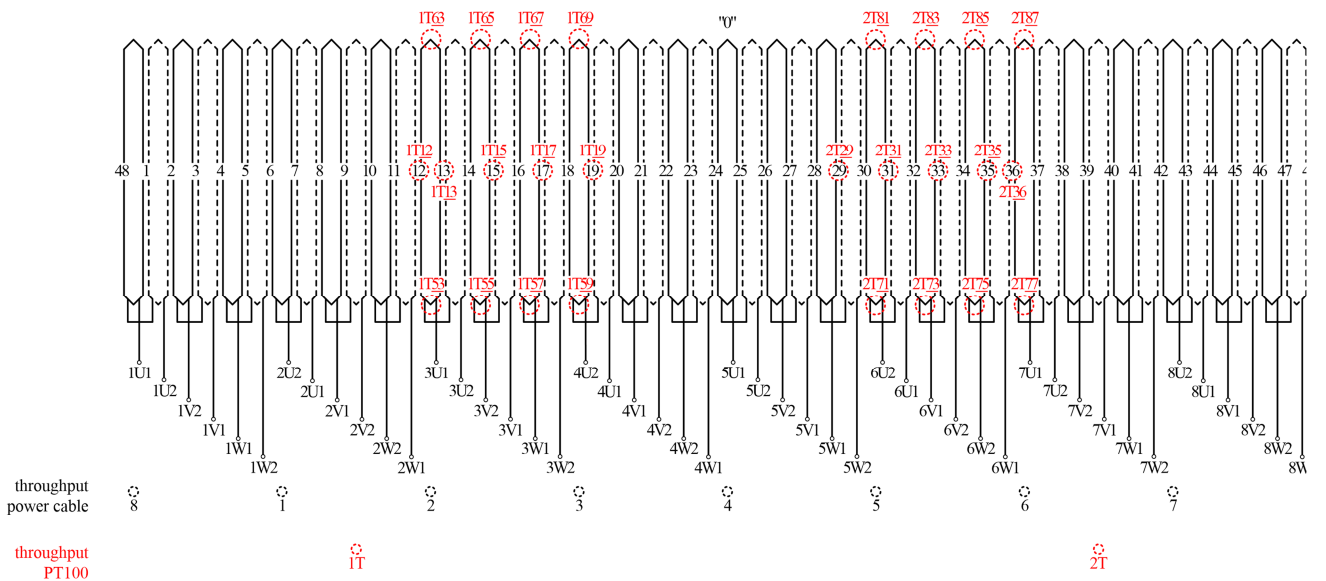


Fig. 11 Winding diagramm with location of PT100-thermistors (red); upper layer (solid); lower layer (dashed); 12 o'clock position marked by "0"



Fig. 12. Linear winder



Fig. 13. Wire feeding with tension control by current-controlled DC-machine and chain drive ($i \approx 2.2$)

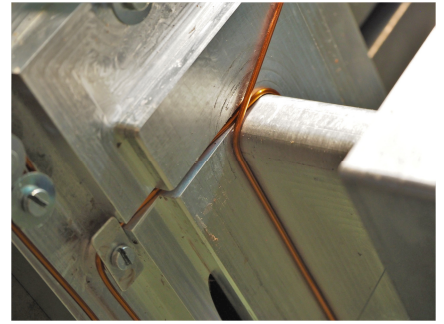


Fig. 14. Initial wire feeding to the winding overhang not affecting the slot winding space; first turn completed

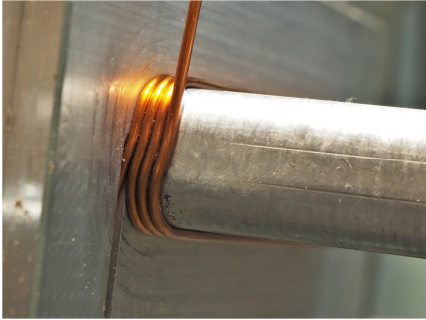


Fig. 15. Turn shift (S-shaped) in the winding overhang leaving the slot winding space unaffected

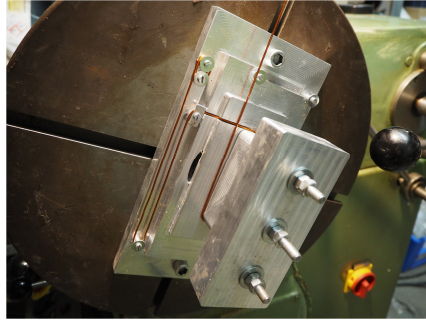


Fig. 16. Winding mould mounted to the main spindle of the winder; wire management on the base plate



Fig. 17. Second layer orthocyclic wound (for demonstration purposes the resin is omitted)

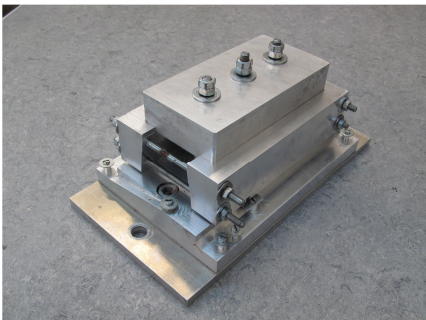


Fig. 18. Lower layer: Assembled mould

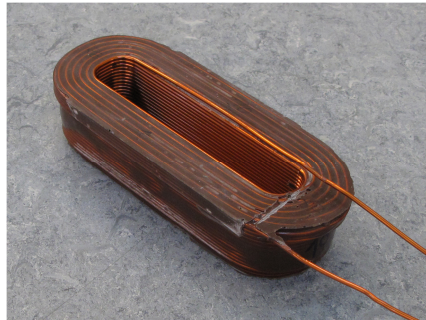


Fig. 19. Lower layer: Prefabricated coil

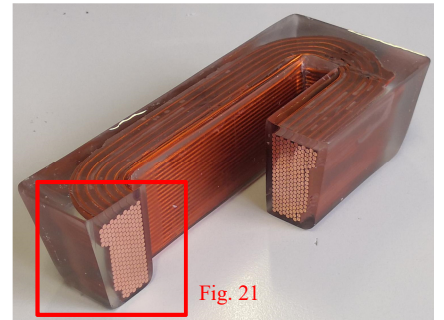


Fig. 20. Lower Layer: Three-quarter-section of coil with polished cut faces (detail in Fig. 21)

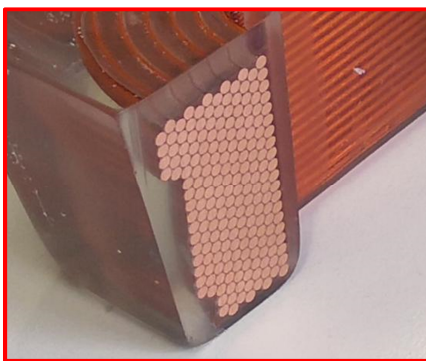


Fig. 21. Lower layer: Polished cut faces in detail; quasi-orthocyclic winding pattern

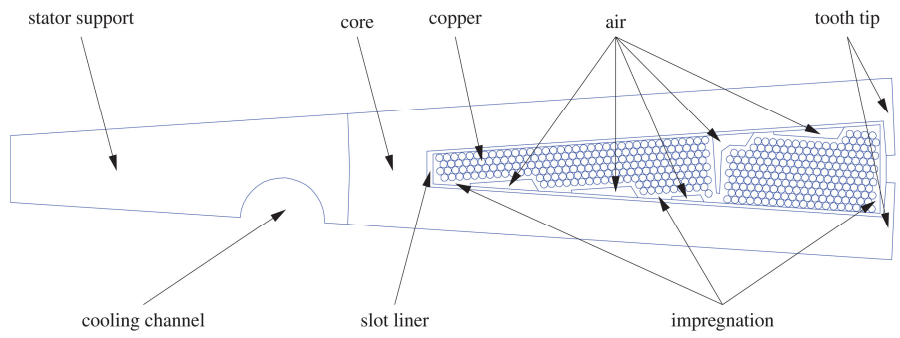


Fig. 22. 2D-thermal-model (FEMM [xii]) [13]

IV. TEST BENCH

For testing and measurement of the prototype the test bench shown in Fig. 24 is configured for a torque up to 5000 Nm. The prototype is coupled via a flange torquemeter, two flexible couplings and a gear box to a PMSM load machine [11]. Both machines will be fed from two voltage link inverters with a shared DC voltage link and with a common active front end (Fig. 25). For electrical and mechanical measurement the data acquisition system *GEN4tB* from *HBK* [ix] is used in combination with *HBK* current-, voltage- and torque-transducers. Since both machines are equipped with water cooling jackets, two independent heat exchanger systems are used enabling individual caloric loss measurements (Fig. 26). The components and suppliers are summarized in Tab. 3.

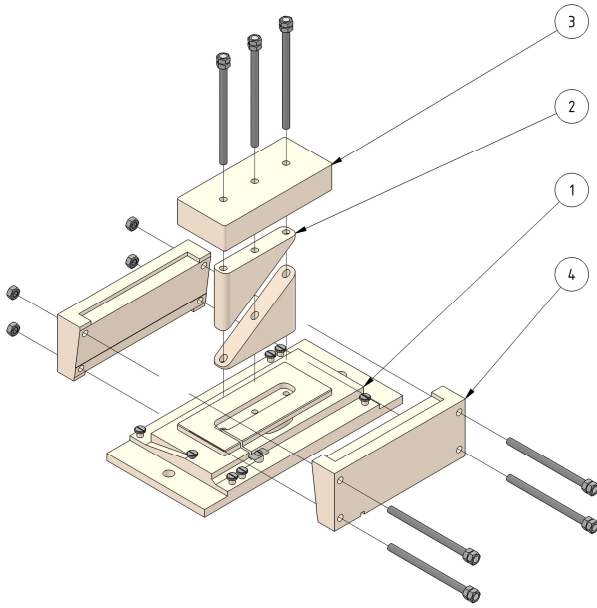


Fig. 23 3D-CAD-model (*Inventor* [i]) of the coil winding mould for the lower layer (exploded view): ① base plate; ② split core; ③ top plate; ④ side mold

TABLE III. TEST BENCH COMPONENTS

Figure	Components	Supplier
Fig. 24: ①	Terminal box	Institute
Fig. 24: ②	Flange mount A	Institute
Fig. 24: ③	Prototype	Institute
Fig. 24: ④	Torquemeter <i>T40B</i> 5 kNM	<i>HBK</i> [ix]
Fig. 24: ⑤	Coupling A: <i>N-ARPEX ARN-6 DEN 203-6</i>	<i>Flender</i> [v]
Fig. 24: ⑥	Gearbox: <i>R137 AD7</i> ($i = 8.71$)	<i>SEW</i> [xv]
Fig. 24: ⑦	Coupling B: <i>ARPEX</i>	<i>Flender</i> [v]
Fig. 24: ⑧	Flange mount B	Institute
Fig. 24: ⑨	load machine	Institute
Fig. 24: ⑩	Test bench	-
Fig. 25	Inverter	<i>Danfoss</i> [iii]
Fig. 26	heat-exchanger	Institute
-	Power Analyser	<i>HBK</i> [ix]

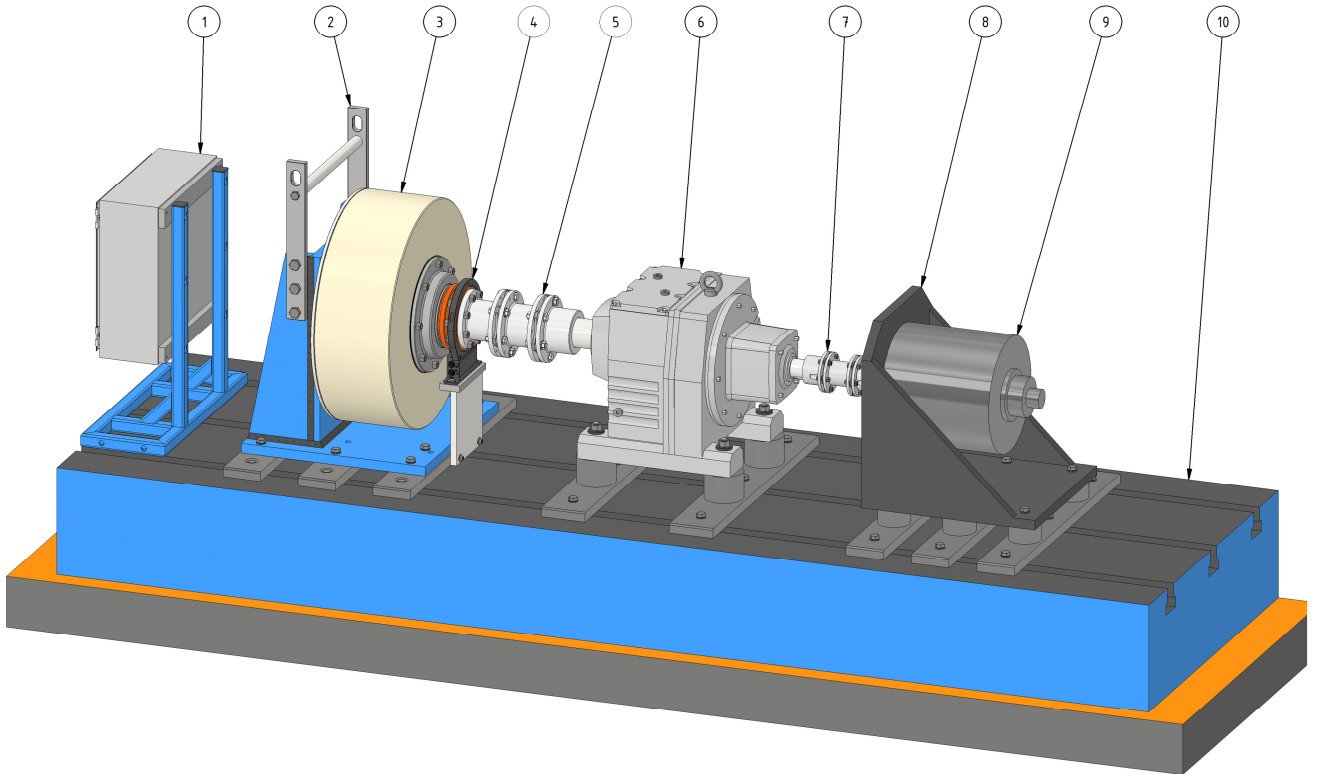


Fig. 24 3D-CAD-model (*Inventor* [i]) of the test bench: ① terminal box; ② flange mount A; ③ prototype machine; ④ torquemeter; ⑤ coupling A; ⑥ gearbox; ⑦ coupling B; ⑧ flange mount B; ⑨ load machine; ⑩ test bench

The machine has an external terminal box (① in Fig. 24) in order to emulate the redundancy operation with a single inverter: In the box the number and circumferential position of fed parallel branches is varied in order to obtain different geometrical feeding patterns. The inactive parallel branches will idle as in a large wind generator operating in redundancy mode. Besides the complete feeding of the machine (Fig. 30), three intermittent feeding patterns (Fig. 27 – 29) are available differing in the width of a fed sector. In the figures fed coils are filled dark and the contour line shows the symmetry group, which is equal to the wavelength of the largest stator field subharmonic.

Especially in this emulated redundancy operation large eddy current losses can occur in the solid rotor yoke due to the (sub-) harmonics evoked by circumferentially intermittent feeding of the stator winding. These losses may lead to unacceptable rotor temperatures for the rare earth permanent magnets. In order to measure the critical rotor temperature a non-contact stationary IR thermometer measures the outer rotor temperature, which is close to the magnet temperature due to the thin rotor yoke.



Fig. 25. Open cabinet of the inverter



Fig. 26. Two water-to-air heat exchanger for prototype and load machine

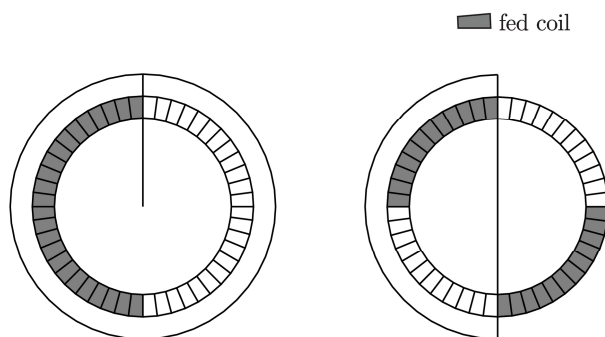


Fig. 27. Redundancy operation pattern: half-circle

Fig. 28. Redundancy operation pattern: two opposing quadrants

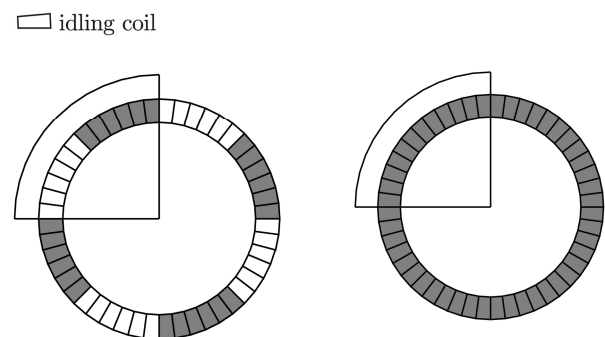


Fig. 29. Redundancy operation pattern: four opposing octants

Fig. 30. Normal operation

V. CONCLUSION

The mechanical design and manufacturing process of a high-torque outer rotor PMSM with tooth-coil-windings and solid rotor yoke was presented and illustrated. The main active components have been designed and manufactured modularly: The stator core is segmented to a yoke ring and 48 tooth packages and the coils are prefabricated and slide on the parallel-sided teeth. This approach is enabled by the tooth-coil winding and leads to an economic manufacturing process by using sub-components (teeth, coils) and the corresponding tools multiple times.

The electromagnetic comparison to a distributed winding in terms of the decrease in the fundamental winding factor, harmonics and length of the winding overhang is not the scope of this paper. But it was shown that this design leads to a relatively high copper fill factor of 0.55 compared to an inserted winding, even though deep and v-shaped slots with a long boundary contour and round wire is used. Further the wet prefabrication of the coils leads to a high resin fill, which improves heat conductivity.

ACKNOWLEDGMENT

This research project is financed by the *Stiftung Energieforschung Baden-Württemberg* founded by *EnBW Energie Baden-Württemberg AG* with the project number A 336 19.

Further we appreciate the support by our industry partners and suppliers. In alphabetical order:

- [i] Autodesk Inc., San Rafael, USA, <http://www.autodesk.com>
- [ii] Brenner GmbH Elektrotechnik, Bürstadt, Germany, <https://brenner-gmbh.de>
- [iii] Danfoss A/S (Vacon), Nordborg, Denmark, <https://www.danfoss.com>
- [iv] Elantas GmbH, Wesel, Germany, <https://www.elantas.com>
- [v] Flender GmbH, Bocholt, Germany, <https://www.flender.com>
- [vi] Fritz Diel Isoliermaterial für die Elektrotechnik GmbH & Co. KG, Dortmund, Germany, <https://www.diel.de>
- [vii] GREMAKO GmbH & Co. KG, Lennestadt, Germany, <https://www.gremako.de>
- [viii] Henke GmbH Zerspanungstechnik, Lampertheim, Germany, <https://www.henke-lampertheim.de>
- [ix] Hottinger Brüel & Kjaer GmbH, Darmstadt, Germany, <https://www.hbm.com>
- [x] JSOL Corporation, Tokyo, Japan, <https://www.jmag-international.com>
- [xi] Magnetworld AG, Jena, Germany, <https://www.magnet-world.de>
- [xii] D. Meeker, FEMM 4.1, USA, <https://www.femm.info>
- [xiii] Nestech, Valdastico, Italy, <https://www.nestech.it>
- [xiv] Schwering & Hasse Elektrodraht GmbH (SHWire), Lügde, Germany, <https://www.sh-wire.de>
- [xv] SEW-EURODRIVE GmbH & Co KG, Bruchsal, Germany, <https://www.sew-eurodrive.de>
- [xvi] SICK AG, Waldkirch, Germany, <https://www.sick.com>
- [xvii] SKF GmbH, Schweinfurt, Germany, <https://www.skf.com/de>
- [xviii] Volkman Elektromaschinenbau GmbH, Werder (Havel), Germany, <https://www.volkman-elmot.de>

REFERENCES

- [1] N. Erd and A. Binder, "Optimal Design of Gearless Permanent Magnet Wind Generators with Tooth-Coil Winding and Solid Rotor

Yoke" (in German: "Optimale Auslegung von getriebelosen, permanentmagneterregten Windgeneratoren mit Zahnspulenwicklung und massivem Rotorjoch"), *Elektrotechnik und Informationstechnik* 137.4-5, 2020, pp. 266-279.

- [2] H. Polinder, M. J. Hoeijmakers and M. Scuotto, "Eddy-current losses in the solid back-iron of PM machines for different concentrated fractional pitch windings", *IEEE Int. Electric Machines Drives Conf.*, Antalya, Turkey, May 2007, pp. 652-657.
- [3] A. Tessarolo, "A survey of state-of-the-art methods to compute rotor eddy-current losses in synchronous permanent magnet machines", *IEEE Workshop on Electrical Machines Design, Control and Diagnosis (WEMDCD)*, Nottingham, UK, Apr. 2017, pp. 12-19.
- [4] G. Ugalde, Z. Q. Zhu, J. Poza and A. Gonzalez, "Analysis of rotor eddy current loss in fractional slot permanent magnet machine with solid rotor back-iron", *XIX Int. Conf. on Electrical Machines (ICEM)*, Rome, Italy, Sept. 2010.
- [5] A. M. EL-Refai, "Fractional-slot concentrated windings synchronous permanent magnet machines: opportunities and challenges", *IEEE Trans. Ind. Electron.* 57.1, pp. 107-121, 2010.
- [6] E. Spooner, A. C. Williamson and G. Catto, "Modular design of permanent-magnet generators for wind turbines", *IEE Proc. Electr. Power Appl.* 143.5, pp. 388-395, 1996.
- [7] Leitner AG (Sterzing, Italy), *Leitwind: Wind Power Plant LTW77*, <http://www.leitwind.com/Products/LTW77-1.500-kW>, visited: 23.05.2020.
- [8] K. Reichert, "Large PMSM with tooth-coil winding, problems, solutions and applications" (in German: "Grosse Synchronmaschinen mit Zahnspulen und Permanentmagneterregung, Problemstellungen, Lösungen und Anwendungen"), *Int. ETG-Kongress*, Düsseldorf, Germany, Oct. 2009.
- [9] N. Erd and A. Binder, "Numerical and analytical analysis of wave harmonics under spatially intermittent feeding", *XXIII. Int. Conf. on Electrical Machines (ICEM)*, Alexandroupolis, Greece, Sept. 2018, pp. 297-303.
- [10] N. Erd and A. Binder, "Eddy currents in solid rotor under spatially intermittent feeding of the stator winding", *XXIII. Int. Conf. on Electrical Machines (ICEM)*, Alexandroupolis, Greece, Sept. 2018, pp. 178-184.
- [11] M. Lehr, "Design and evaluation of electrical machines with stator permanent magnets with high torque density" (in German: "Auslegung und Bewertung elektrischer Maschinen mit Permanentmagneten im Stator für hohe Drehmomentdichten"), *Diss. TU Darmstadt*, Darmstadt, 2020.
- [12] N. Erd and A. Binder, "Concentrated Windings for Wind Generators with Solid Rotor Iron and Redundant Feeding", *XXIV. Int. Conf. on Electrical Machines (ICEM)*, Gothenburg, Sweden, Aug. 2020, pp. 2596-2602.
- [13] N. Erd and A. Binder, "Scaled Prototype of a Redundantly Fed, Gearless PMSM Wind Generator with Tooth Coil Winding and Solid Rotor Yoke", *VDE Antriebssysteme*, Munich, Germany, Nov. 2021, to be published.

BIOGRAPHIES

Nicolas Erd (born in 1989 in Berlin, Germany) received his B.Sc. and M.Sc. in Elect. Eng. from TU Berlin in 2013 and 2015. Since 2015 he is with the Institute of Electrical Energy Conversion at the TU Darmstadt as a research assistant concentrating on large PMSM for wind turbines.

Andreas Binder Senior Member IEEE, Member VDE, IET, VDI, EPE, received the degrees Dipl.-Ing. (diploma) and Dr. techn. (PhD) for Electrical Engineering from the University of Technology, Vienna/Austria, in 1981 and 1988. He worked in industry from 1981 to 1983 at ELINUnion AG, Vienna, on large synchronous generator design and from 1989 to 1997 as a group leader for developing DC and inverter-fed AC motors and drives at Siemens AG, Bad Neustadt and Erlangen, Germany. Since 1994 he is lecturer (habilitation) at University of Technology, Vienna/Austria, and since 1997 he is Head of the Institute of Electrical Energy Conversion, Darmstadt University of Technology, as a full professor. Research topics are high speed motors, permanent magnet E-Machines, bearing currents, drive technologies for hybrid and electric cars, drive systems for electric railways, magnetic suspension and magnetic bearings, generator systems e.g. for renewable energies.